Detecting Changes in Boundary Conditions based on Sensitivity-based Statistical Tests

Alexander Mendler, Michael Döhler, Falk Hille

NDT-CE 2022 - The International Symposium
on Nondestructive Testing in Civil Engineering
Zurich, Switzerland, August 16-18, 2022

Detecting Changes in Boundary Conditions based on Sensitivity-based Statistical Tests

Alexander MENDLER[1]*, Michael DÖHLER[2], Falk HILLE[3]

[1] TUM School of Engineering and Design, Technical University of Munich, Munich, Germany
[2] Univ. Gustave Eiffel, Inria, COSYS/SII, I4S, Rennes, France
[3] BAM Federal Institute for Materials Research and Testing, Division Buildings and Structures, Berlin, Germany
*Corresponding author, e-mail address: *alexander.mendler@tum.de*

Abstract
Structural health monitoring is a promising technology to automatically detect structural changes based on permanently installed sensors. Vibration-based methods that evaluate the global system response to ambient excitation are suited to diagnose changes in boundary conditions, i.e., changes in member prestress or imposed displacements. In this paper, these changes are evaluated based on sensitivity-based statistical tests, which are capable of detecting and localizing parametric structural changes. The main contribution is the analytical calculation of sensitivity vectors for changes in boundary conditions (i.e., changes in prestress or support conditions) based on stress stiffening, and the combination with a numerically efficient algorithm, i.e., Nelson's method. One of the main advantages of the employed damage diagnosis algorithm is that, although it uses physical models for damage detection, it considers the uncertainty in the data-driven features, which enables a reliability-based approach to determine the probability of detection. Moreover, the algorithm can be trained and the probability of detecting future damages can be predicted based on data and a model from the undamaged structure, in an unsupervised learning mode, making it particularly relevant for unique structures, where no data from the damaged state is available. For proof of concept, a numerical case study is presented. The study assesses the loss of prestress in a two-span reinforced concrete beam and showcases suitable validation approaches for the sensitivity calculation.

Keywords: Global ambient vibrations, asymptotic local approach, sensitivity vectors, probability of detection, stress stiffening, Nelson's method

1 Introduction

Increasingly, periodic inspections based on non-destructive testing are supplemented with structural health monitoring (SHM) systems, which monitor structures based on permanently installed sensors and online damage diagnosis algorithms. Global vibration-based methods have the advantage that a few sensors suffice to monitor large structures. What is more, no activators are required on-site, as the ambient excitation may be sufficient, and the methods can be applied during normal operating conditions. The engineering community appears to agree that global vibration-based methods may be insensitive to detect small and local damages, especially for sudden failure mechanisms such as fatigue phenomena, but they are a promising technology for the monitoring of external prestressing tendons or cables [1] and changes in support conditions. While extensive research efforts have been made since the 1990s to advance global vibration-based methods, only few instances are reported yet where monitoring systems lead to an economic benefit. One reason for this may be that only a few tools are available to assess the performance of monitoring systems before they are installed and to optimize them accordingly.

This paper proposes a new tool to analyze changes in prestress and support conditions based on global vibration-based features, such as natural frequencies and mode shapes. The method is based on sensitivity-based statistical tests, which are capable of detecting [2], localizing [3],

and quantifying structural damage. The employed features may be time-domain-based, such as the subspace-based residual [2], the robust subspace-based residual [4], or the Hankel matrix difference [5], or directly be based on natural frequencies and mode shapes [6]. If evaluated in combination with physical models, it allows one to draw probability of detection (POD) curves based on measurement data from the undamaged structure [7], and therefore, assess the probability of detection before damage occurs. The objective of this paper is to extend the method, so it can be applied for the monitoring of boundary conditions, especially of large engineering systems with ten thousands of degrees of freedom.

The paper is organized into four additional sections: Section 2 recaps sensitivity-based statistical tests as well as the existing approach to determine analytical POD curves. Section 3 elaborates on the sensitivity computation for changing boundary conditions and helps the reader get an overview of appropriate approaches for the sensitivity computation. Section 4 showcases a proof of concept study based on a numerical two-span reinforced concrete beam, including a discussion on the practicality of the presented approaches to compute the sensitivity vectors. Ultimately, Section 5 concludes the paper highlighting the main contribution and future research topics.

2 Damage Detection

This section revisits a damage diagnosis algorithm that allows one to predict the POD for future damage scenarios without any data from the damaged structure. The method is based on sensitivity-based statistical tests. The tests evaluate data-driven residual vectors, i.e., vectors that indicate the presence of damage through deviations of any vector entry from zero, and link them to changes in model-based structural parameters using sensitivity vectors.

2.1 Data-driven Residual

The residual vector is estimated based on data. In this article, a combined frequency and mode shape-based residual vector is considered, where all mode shapes are normalized to unit displacement. The residual $\boldsymbol{r} \in \mathbb{R}^{N_f}$ is defined as

$$\boldsymbol{r} = \begin{bmatrix} \hat{\boldsymbol{f}} - \hat{\boldsymbol{f}}^0 \\ \mathrm{vec}\left(\hat{\boldsymbol{U}} - \hat{\boldsymbol{U}}^0\right) \end{bmatrix}, \tag{1}$$

where $\hat{\boldsymbol{f}} \in \mathbb{R}^m$ is the estimated frequency vector and $\hat{\boldsymbol{U}} \in \mathbb{R}^{(r-1)\times m}$ is the mode shape matrix with r sensor locations and m modes of vibration. The normalized mode shape coordinate is always one and carries no damage-related information, which is why the number of rows of the mode shape matrix is reduced by one. The superscript $(\cdot)^0$ indicates that the values are taken from a reference data set and vec$(\cdot)$ is the vectorization operator that stacks each column in the mode shape matrix $\hat{\boldsymbol{U}}$. All modal parameters are estimated based on operational modal analysis (OMA), using covariance-driven subspace-based system identification (SSI-Cov); thus the residual in Eq. (1) has an asymptotically Gaussian distribution. State-of-the-art OMA algorithms [8] also estimate the covariance matrix $\boldsymbol{\Sigma} \in \mathbb{R}^{N_f \times N_f}$, which is calculated as

$$\boldsymbol{\Sigma} = \frac{\mathrm{N}^0}{\mathrm{n_b} - 1} \sum_{k=1}^{n_b} \boldsymbol{r}_k \boldsymbol{r}_k^T, \tag{2}$$

where N^0 is the number of data points in the reference state and n_b is the number of blocks. The method described in the subsequent section is not limited to modal parameters and can also be applied to other residual formulations, such as the classic subspace-based residual [2], the robust subspace-based residual [4], the Hankel matrix difference [5], and others.

2.2 Model-based Detection

Sensitivity-based statistical tests allow one to evaluate the residual vector from Eq. (1) with respect to structural parameters in physical models, meaning it can be tested how likely it is that structural parameters have changed. First of all, the anticipated damage scenarios have to be parameterized, meaning all structural parameters that manifest damage are stored in a monitoring vector $\boldsymbol{\theta} \in \mathbb{R}^H$. In recent publications, this vector included material constants and cross-sectional values (such as the cross-sectional area, or the bending stiffness). This paper will incorporate internal forces and support displacements for the first time. The employed test statistic for change detection on Gaussian residuals is defined as [2]

$$t = N \cdot \mathbf{r}^{\boldsymbol{T}} \boldsymbol{\Sigma}^{-1} \boldsymbol{\mathcal{J}} \cdot (\boldsymbol{\mathcal{J}}^T \boldsymbol{\Sigma}^{-1} \boldsymbol{\mathcal{J}}) \cdot \boldsymbol{\mathcal{J}}^{\boldsymbol{T}} \boldsymbol{\Sigma}^{-1} \boldsymbol{r}, \tag{3}$$

where N is now the number of data points in the tested data set, $\boldsymbol{\Sigma}$ is the covariance matrix, and $\boldsymbol{\mathcal{J}} \in \mathbb{R}^{N_f \times H}$ is the sensitivity matrix. The sensitivity matrix is typically evaluated based on a physical model of the structure and contains the first-order derivatives of the mean residual vector with respect to the structural parameter vector

$$\boldsymbol{\mathcal{J}} = \left. \frac{\delta E_{\boldsymbol{\theta}}[\boldsymbol{r}]}{\delta \boldsymbol{\theta}} \right|_{\boldsymbol{\theta}=\boldsymbol{\theta}^0}, \tag{4}$$

but more on this follows in the next sections. To detect damage, the test statistic from Eq. (3) is compared against a safety threshold value t_{thres} which can be set, for example, based on the allowable false alarm rate α in the reference state, i.e., the relative number of tests beyond the safety threshold if no damaged has occurred.

2.3 Probability of Detection

Due to unknown loads, measurement noise, and other sources of uncertainty, the test statistic from Eq. (3) is scattered. Its derivation assumes that the residual can be approximated by a normal distribution, and consequently, the test statistic t can be approximated by a $\chi^2(\nu, \lambda)$-distribution with ν degrees of freedom and non-centrality λ (the mean test response). If it is assumed that the change is restricted to a single parameter h, and if this change is known $\Delta\theta_h = \theta_h - \theta_h^0$, the mean test response λ can be calculated analytically through [9]

$$\lambda = \mathrm{N}\left(\theta_h - \theta_h^0\right)^2 F_{hh}, \tag{5}$$

where $F_{hh} = \boldsymbol{\mathcal{J}}_h^T \boldsymbol{\Sigma}^{-1} \boldsymbol{\mathcal{J}}_h$ is the Fisher information, calculated based on the h-th column in the sensitivity matrix. On close inspection of Eq. (5), it can be appreciated that the test response to damage can be "predicted" based on quantities that are available in the undamaged state of the structure without having to analyze data from the damaged structure.

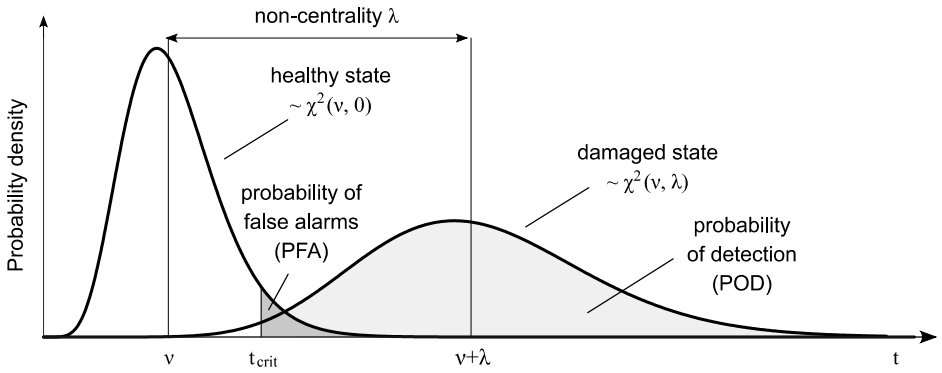

Figure 1: Distribution of the statistical test

In summary, the distribution in the undamaged state can be described through a mathematical probability density function (PDF) $\chi^2(\nu, 0)$, the safety threshold t_{thres} is set based on the allowable false alarm rate, and the mean test response λ to future damage is known, yielding the test distribution in the damaged state $\chi^2(\nu, \lambda)$, see Figure 1. That means that the POD could be calculated as the area below the damaged state PDF

$$\mathrm{POD}(\lambda) = \int_{t_{thres}}^{\infty} f_{\chi^2(\nu,\lambda)}(t)\, dt. \tag{6}$$

In other words, the POD can be mathematically linked to the non-centrality in Eq. (5), and thus, the parameter change $\Delta\theta_h = \theta_h - \theta_h^0$. Hence, POD curves can be created by drawing the POD against the parameter change $\Delta\theta_h$ [7]. The next section will explain what modification have to be made to extend this approach to changes in boundary conditions.

3 Modal Sensitivities

The previous section explains how to evaluate the POD for changes in material constants and cross-sectional values. To the authors' knowledge, this approach has never been employed to monitor varying level of prestress, and this section proposes an approach to compute the corresponding sensitivity matrix. In the first subsection, the underlying dynamic system is recapped. Secondly, it is shown how the effect that changing prestressing levels have on modal parameters can be modelled in finite element software, and ultimately, various computation approaches are compared to analytically evaluate the modal derivatives.

3.1 Eigenvalue Problem

All following considerations are based on a dynamic system with n degrees of freedom and symmetrical matrices for the mass $\boldsymbol{M}$, stiffness $\boldsymbol{K}$, and damping $\boldsymbol{C}$. In that case, the equation of motion can be written as follows

$$\left(s_i^2\boldsymbol{M} + s_i\boldsymbol{D} + \boldsymbol{K}\right)\boldsymbol{u_i} = \boldsymbol{F}\boldsymbol{u_i} = \boldsymbol{0}, \tag{7}$$

where s_i and $\boldsymbol{u_i}$ are the complex-valued eigenvalues and eigenvectors, and $\boldsymbol{F} = s_i^2\boldsymbol{M} + s_i\boldsymbol{D} + \boldsymbol{K}$ is a matrix that is introduced here to simplify the notations later on. Eigenvectors are not unique

in the sense that any scalar multiple of an eigenvector is also an eigenvector. For undamped systems, it is common to normalize mode shapes to unit mass and for damped systems, a common normalization is $\boldsymbol{u}_i^T(2s_i\boldsymbol{M}+\boldsymbol{D})\boldsymbol{u}_i = 1$, which ensures that eigenvectors have equivalent scaling to measured eigenvectors [10]. After rewriting the system as follows

$$\boldsymbol{A} = \begin{bmatrix} -\boldsymbol{K} & \boldsymbol{0} \\ \boldsymbol{0} & \boldsymbol{M} \end{bmatrix}, \qquad \boldsymbol{B} = \begin{bmatrix} \boldsymbol{C} & \boldsymbol{M} \\ \boldsymbol{M} & \boldsymbol{0} \end{bmatrix}, \tag{8}$$

the eigenvalue problem $\boldsymbol{AU} = \boldsymbol{BUS}$ can be solved and the complex-valued poles in $\boldsymbol{S} = \mathrm{diag}(s_1, s_1^*, \dots, s_n, s_n^*)$ and mode shapes $\boldsymbol{U} = [\boldsymbol{u}_1, \boldsymbol{u}_1^*, \dots, \boldsymbol{u}_n, \boldsymbol{u}_n^*]$ can be determined. Ultimately, the modal frequencies and damping ratios can be calculated as

$$f_i = \frac{1}{2\pi}\sqrt{\mathrm{real}(s_i)^2 + \mathrm{imag}(s_i)^2}, \qquad \zeta_i = -\frac{\mathrm{real}(s_i)}{2\pi f_i}. \tag{9}$$

3.2 Stress Stiffening

Axial member forces and imposed displacements, intended or accidental, alter the initial stress state in structures and the resulting modal parameters. The effect is known as *stress stiffening* and it causes stabilizing or destabilizing effects within the structure. A straightforward way to model such effects in finite element software is through a geometric stiffness matrix $\boldsymbol{K}_{geo}$, which is added to the elastic stiffness matrix $\boldsymbol{K}_{el}$, and depends on the axial member forces $\boldsymbol{p}$,

$$\boldsymbol{K} = \boldsymbol{K}_{el} + \boldsymbol{K}_{geo}(\boldsymbol{p}). \tag{10}$$

This approach is particularly advantageous for large structures where no non-linear calculations are desired. It is only accurate for small displacements, small strains, and leads to no update of the geometry, so the mass matrix remains unchanged [11]. Subsequently, modal parameters can be determined as explained in Section 3.1. More precisely, the geometric stiffness matrix is added to the elastic stiffness in local element coordinates before transforming the matrices into the global coordinates. This way, the prestressing forces can directly be applied to the respective element matrices. The shape of the local stiffness matrix depends on the type of elements being used (beams, shells, solids, etc.), with typical examples in [11].

If imposed displacements are the cause of internal stresses, a static structural analysis has to be performed first to obtain the global stress vector. In the next step, the force vector is transformed onto element level, the geometric stiffness is evaluated, and back-transformed onto global coordinates. Ultimately, a dynamic analysis is run to solve for the modal parameters under consideration of the geometric stiffness terms. To determine the global force vector, the displacement vector is split into free degrees of freedom $\boldsymbol{u}_a$ and fixed degrees of freedom $\boldsymbol{u}_b$ with the corresponding matrix equation of motion (neglecting damping)

$$\begin{bmatrix} \boldsymbol{M}_{aa} & \boldsymbol{M}_{ab} \\ \boldsymbol{M}_{ba} & \boldsymbol{M}_{bb} \end{bmatrix}\begin{bmatrix} \ddot{\boldsymbol{u}}_a \\ \ddot{\boldsymbol{u}}_b \end{bmatrix} + \begin{bmatrix} \boldsymbol{K}_{aa} & \boldsymbol{K}_{ab} \\ \boldsymbol{K}_{ba} & \boldsymbol{K}_{bb} \end{bmatrix}\begin{bmatrix} \boldsymbol{u}_a \\ \boldsymbol{u}_b \end{bmatrix} = \begin{bmatrix} \boldsymbol{p}_a \\ \boldsymbol{p}_b \end{bmatrix}. \tag{11}$$

For a static support displacement, the first line can be reformulated to $\boldsymbol{M}_{aa}\ddot{\boldsymbol{u}}_a + \boldsymbol{K}_{aa}\boldsymbol{u}_a = \boldsymbol{p}_a - \boldsymbol{K}_{ab}\boldsymbol{u}_b$ as accelerations are zero at the fixed supports. In other words, the permanent support

displacement is modelled through an equivalent force $-\boldsymbol{K}_{ab}\boldsymbol{u}_b$ due to static displacements at the free degrees of freedom [11]. Damping does not have to be considered because the velocity at the fixed supports is zero. In global coordinates, a new force vector can be defined that includes both prestressing forces and support displacements

$$\boldsymbol{p} = \boldsymbol{p}_a - \boldsymbol{K}_{ab}\boldsymbol{u}_b, \tag{12}$$

and the prestressed modal analysis can be conducted as described in Section 3.1.

3.3 Modal Derivatives

The goal of this paper is to analyze changes in prestress based on changes in natural frequencies and mode shapes, and to discuss different approaches for the sensitivity computation. Hence, the structural parameter vector is populated with axial member forces $\boldsymbol{\theta} = [\theta_1, \theta_2, \dots]^T$ and the data-driven residual vector takes the form from Eq. (1). Since the derivatives are calculated based on a numerical model (and not based on operational modal analysis), the hat symbol is dropped for modal parameters in the following notations and the sensitivity matrix is

$$\boldsymbol{\mathcal{J}} = \begin{bmatrix} \frac{\delta f_1}{\delta \theta_1} & \frac{\delta f_1}{\delta \theta_2} & & \frac{\delta f_1}{\delta \theta_H} \\ \vdots & \vdots & & \vdots \\ \frac{\delta f_m}{\delta \theta_1} & \frac{\delta f_m}{\delta \theta_2} & & \frac{\delta f_m}{\delta \theta_H} \\ \frac{\delta \boldsymbol{u}_1}{\delta \theta_1} & \frac{\delta \boldsymbol{u}_1}{\delta \theta_2} & \cdots & \frac{\delta \boldsymbol{u}_1}{\delta \theta_H} \\ \vdots & \vdots & & \vdots \\ \frac{\delta \boldsymbol{u}_m}{\delta \theta_1} & \frac{\delta \boldsymbol{u}_m}{\delta \theta_2} & & \frac{\delta \boldsymbol{u}_m}{\delta \theta_H} \end{bmatrix}. \tag{13}$$

The *finite different method* is one of the most straightforward approaches for the sensitivity computation. To compute the first-order derivatives, as many finite element analysis runs have to be performed as there are structural parameters in $\boldsymbol{\theta}$. For each parameter, a perturbation $\Delta\theta_j$ is applied, and the frequencies and mode shapes are extracted before and after the structural changes. Consequently, the derivatives can be calculated as

$$\frac{\delta f_i}{\delta \theta_j} = \frac{f_i - f_i^0}{\theta_j - \theta_j^0}, \tag{14}$$

$$\frac{\delta \boldsymbol{u}_i}{\delta \theta_j} = \frac{1}{\theta_j - \theta_j^0}\left(\boldsymbol{u}_i - \boldsymbol{u}_i^0\right). \tag{15}$$

Nelson's method is an alternative approach to computing modal derivatives. In the literature [12], the modal derivatives are given with respect to the poles s_i with

$$\frac{\delta s_i}{\delta \theta_j} = -\boldsymbol{u}_i^T \left(s_i^2 \frac{\delta \boldsymbol{M}}{\delta \theta_j} + s_i \frac{\delta \boldsymbol{C}}{\delta \theta_j} + \frac{\delta \boldsymbol{K}}{\delta \theta_j} \right) \boldsymbol{u}_i, \tag{16}$$

and by applying the chain rule to Eq. (9), the frequency derivatives yield

$$\frac{\delta f_i}{\delta \theta_j} = \frac{1}{2\pi\,|s|}\left(\text{real}(s_i)\text{real}\left(\frac{\delta s_i}{\delta \theta_j}\right) + \text{imag}(s_i)\text{imag}\left(\frac{\delta s_i}{\delta \theta_j}\right)\right). \tag{17}$$

The mode shape derivatives, on the other hand, are defined as

$$\frac{\delta \boldsymbol{u}_i}{\delta \theta_j} = \boldsymbol{x}_i + c_i \boldsymbol{u}_i. \tag{18}$$

The factor c_i is a scaling constant and $\boldsymbol{x}_i$ the solution of the following equation

$$\begin{bmatrix} \boldsymbol{F}_{i11} & 0 & \boldsymbol{F}_{i13} \\ 0 & 1 & 0 \\ \boldsymbol{F}_{i13} & 0 & \boldsymbol{F}_{i33} \end{bmatrix} \begin{bmatrix} \boldsymbol{x}_{i1} \\ x_{i2}(=0) \\ \boldsymbol{x}_{i3} \end{bmatrix} = \begin{bmatrix} \boldsymbol{h}_{i1} \\ 0 \\ \boldsymbol{h}_{i3} \end{bmatrix}, \tag{19}$$

$$\boldsymbol{h} = \left(s_i^2 \frac{\delta \boldsymbol{M}}{\delta \theta_j} + \frac{\delta \boldsymbol{K}}{\delta \theta_j}\right)\boldsymbol{u}_i + (2s_i \boldsymbol{M} + \boldsymbol{C})\boldsymbol{u}_i \frac{\delta s_i}{\delta \theta_j},$$

where the zeroed-out row and column correspond to the degree of freedom with the maximum mode shape amplitude of $\boldsymbol{u}_i$. Ultimately, the scaling constant can be determined as

$$c_i = -\boldsymbol{u}_i^T (2s_i \boldsymbol{M} + \boldsymbol{D})\boldsymbol{x}_i - \frac{1}{2}\boldsymbol{u}_i^T \left(2\boldsymbol{M}\frac{\delta s_i}{\delta \theta_i} + 2s_i \frac{\delta \boldsymbol{M}}{\delta \theta_j} + \frac{\delta \boldsymbol{D}}{\delta \theta_j}\right)\boldsymbol{u}_i. \tag{20}$$

4 Application

For proof of concept, a numerical case study is performed, where varying levels of prestress are analysed based on data-driven changes in natural frequencies and mode shapes. The objective is to analyse measurement data from the undamaged structure in order to predict the POD curves. Secondly, the predictions are validated based on data from the damaged state, and ultimately, the different approaches to calculating the modal derivatives are critically discussed.

4.1 Description

The structure under consideration is a two-span reinforced concrete beam. It is a double-symmetrical structure with a length of 24 m and a width of 90 cm. The cross section consists of an inverted u-shaped beam with two external prestressing tendons that are anchored through vertical anchorage plates at both abutments, see Figure 2. The beam is supported on a total of six elastomer bearings, two at either support. The material properties are summarized in Table 1. The structure is a numerical model of a full-scale laboratory beam at the BAM[1] research centre in Berlin, also known as the BLEIB structure; however, all following considerations are based on numerically generated data from a non-calibrated finite element model.

[1] Federal Institute for Materials Research and Testing, www.bam.de

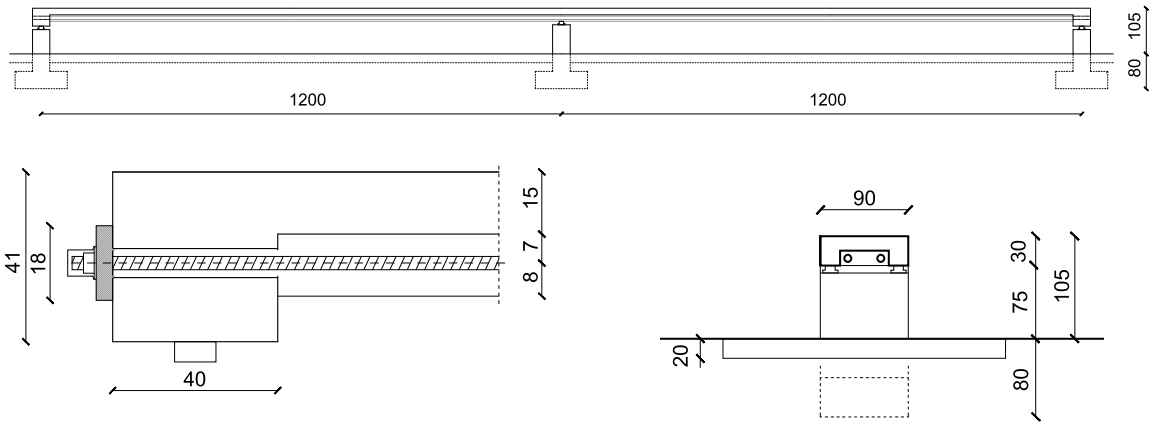

Figure 2: Technical drawings of the two-span reinforced concrete beam including the longitudinal section (top), anchor detail (bottom left), and cross section (bottom right).

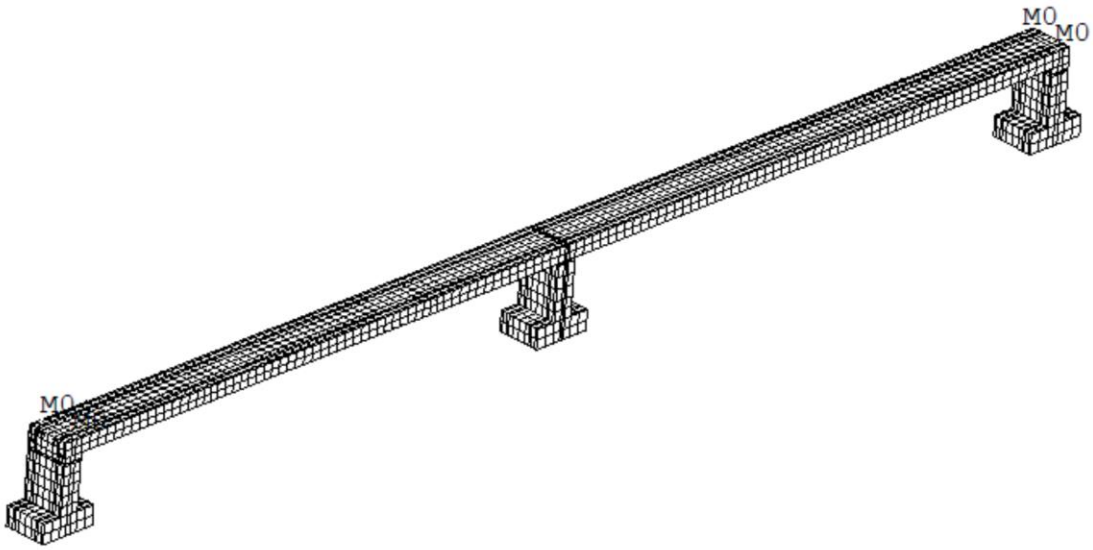

Figure 3: ANSYS Finite element model with 12,124 degree of freedom

Table 1: Material properties and element types

Component	Material	Element type	E-modulus	Mass
Superstructure	C45/55	SOLID185	36,000 MN/m^2	2,450 kg/m^3
Bearings	Gumba Typ C (2) 100 x 100 x 49	SOLID185	2,000 MN/m^2	934 kg/m^3
Substructure	C25/30	SOLID185	36,000 MN/m^2	2,450 kg/m^3
Pretension rods	Dywidag 32 WR	-	-	-
Reinforcements	varying	Discrete REINF	210,000 MN/m^2	7,750 kg/m^3

The numerical model is built in ANSYS using solid elements for the concrete of the superstructure and the substructure, discrete reinforcement elements, and solid elements for the elastomer pads. The pretension rods are modelled through an equivalent horizontal force on the anchorage plates and point masses. For simplification, only linear isotropic material models are used, characterized by the material properties in Table 1. The soil is assumed to have infinite

stiffness, and all nodes on the element surfaces below grade are fixed. Damage is parameterized through uniform changes in prestress in both longitudinal tendons. That means a single structural parameter is monitored which, in the reference configuration, is a longitudinal force of $\theta = 300$ kN. The analysis of the beam is split into two solution states. First a structural analysis is performed to apply the internal forces, and secondly, a prestressed modal analysis is run. In total, the model exhibits 8,474 nodes and 14,124 degrees of freedom, see Figure 3.

The damage diagnosis is implemented in MATLAB. The interface between MATLAB and ANSYS is set up based on the MATLAB aaS Toolbox, where MATLAB forwards the structural parameter vector $\boldsymbol{\theta}$ to ANSYS, which in turn builds the models, solves the static analysis, and the prestressed modal analysis, and returns the system matrices $\boldsymbol{M}, \boldsymbol{C}, \boldsymbol{K}$ as well as the modal parameters. The sensitivity computation is conducted in MATLAB and so is the vibration generation based on a modal reduction approach. Moreover, an operational modal analysis algorithm is implemented to extract the modal parameters as well as their covariance matrix from the generated records, see Table 2 for more details on the signal processing parameters.

The instrumentation consists of 12 velocimeters that measure the vibration in the centre line of the beam and in the vertical direction, where the x-coordinates are shown in Figure 4 (right). For excitation, Gaussian white noise is input in the same direction as the outputs are measured and moreover, uniformly distributed noise with a maximum magnitude of 5% of the output's standard deviation is added to the generated data sets to simulate measurement noise. The stabilization diagram from the SSI-Cov and the observed modes of vibration are shown in Figure 4. In this study, only the first two vertical modes of vibration are considered and a modal damping ratio of 2% critical damping is assumed.

4.2 Undamaged State

The method described in Section 2 allows one to predict POD curves based on data from the undamaged structure, which is now done for the two-span beam. First, a 30 min-long meas–urement record is generated for the undamaged structure. Secondly, the natural frequencies and mode shapes are extracted from this record together with the covariance matrix [8]. Where the covariance matrix is estimated based on data, the Jacobian matrix is computed based on the physical model. With the Jacobian and the covariance matrix at hand, the Fisher information can be calculated and the number of degrees of freedom of the χ^2 −distribution can be calculated to $\nu = \text{rank}(\boldsymbol{\mathcal{J}}^T \boldsymbol{\Sigma}^{-1} \boldsymbol{\mathcal{J}}) = 1$. The last required quantity for the computation of the POD curves is the safety threshold t_{thres}. In this case, it is calculated based on a desired false alarm rate of 5% in the undamaged state, meaning it is acceptable that one out of 20 tests is beyond the safety threshold in the undamaged state.

To verify the theoretical considerations from above, another 100 data sets are generated in the undamaged state, the modal parameters are extracted and the test statistic is evaluated for each record. By drawing the distribution of the test statistic in Figure 5 (right), it can be appreciated that the distribution's mean is equal to $\mu_{\chi^2} = \nu = 1.5$, which is close to the theoretical value.

Table 2: Signal processing parameters

Signal generation		Signal processing	
Excitation	Gaussian white noise	Downsampling	-
Measurement noise	Uniform white noise	Filtering	-
Noise level	5% of output variance	System order n	14
Measurement type	Velocity	Time lag parameters	20
Sampling frequency	50 Hz	Number of blocks n_b	500
Duration in reference state	30 min + 100 x15 s		
Duration in damaged state	100 x 15 s		

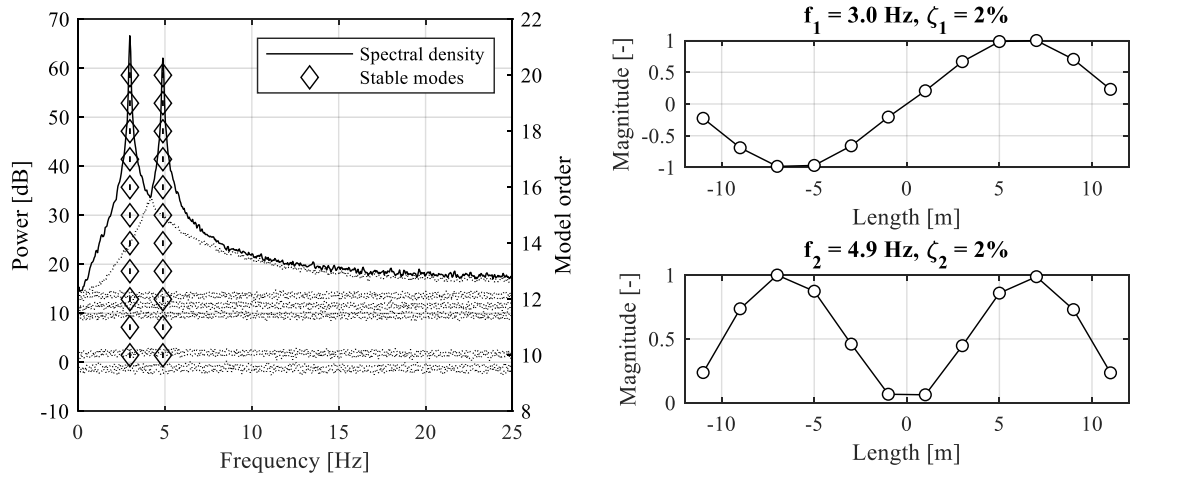

Figure 4: Stabilization diagram for the SSI-Cov (left) and corresponding modes of vibration (right)

The POD curve is now drawn for varying levels of prestress. Figure 5 (left) shows the POD curve for relative parameter changes between 0 and 3%. Based on this preliminary analysis, a parameter change is barely detectable if the parameter change is below 0.1% (0.3 kN), and the POD is close to 100% for parameter changes larger than 2.5% (7.5 kN). Reducing the pretension in both tendons by 1.5% (4.5 kN), on the other hand, leads to a POD of 80%.

4.3 Damaged State

This section attempts to validate the analytical POD curves through empirical simulations. That means, the prestress in both tendons is relaxed by 1.5% and another 100 measurement records are created in the damaged state. Then, modal parameters are extracted, using operational modal analysis, and the test statistic is evaluated for each record using the covariance and the Jacobian from the reference structure.

As before, the distribution of the test statistic is drawn in Fig. 2, and the relative number of tests beyond the safety threshold (in the damaged state, this value is the empirical POD) is counted. After comparing the analytical POD from the POD curve in Figure 5 (left) to the empirical POD in Figure 5 (right), the validation study can be concluded, because the values of 80% and 79.5% are almost identical, so the POD curves and the sensitivity matrices are accurate.

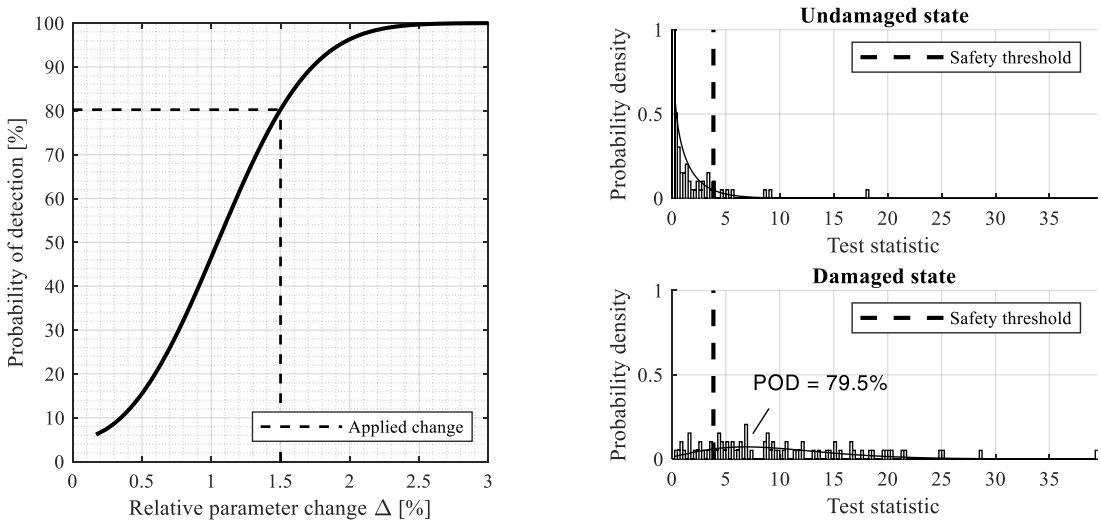

Figure 5: Analytical probability of detection curve (left) and empirical test distribution before and after a loss of prestress (right).

4.4 Discussion

Vibration-based approaches are sometimes criticized, especially for bridge monitoring, due to their alleged low sensitivity to small and local damages. This article not only proposes an approach to explicitly quantify the damage detectability but also suggests that vibration-based methods may be appropriate for the monitoring of boundary conditions, i.e., prestress in external tendons or support conditions. The authors are aware that, when applied to large engineering structures, such as bridges, the success of the method hinges on a practical computation of the sensitivity matrix, which is why the different approaches are discussed in the following.

A major downside of the finite difference method is that the results depend on the step size $\Delta\theta$. The Nelson method, on the other hand, does not depend on the step size and leads to accurate derivatives if the local stiffness matrix is proportional to the monitored parameter, which is the case for the Young's modulus E, axial member forces p, or stiffness pre-multipliers. However, applying the approach to the monitoring of geometric properties such as the member length L, or cross-sectional values such as the area A and the moment of inertia I, will introduce bias in the sensitivity, alleviating the advantages of Nelson's method. What is more, Nelson's method requires the mass, stiffness, and damping matrix as inputs as well as the observed eigenvectors at all degrees of freedom of the numerical model. Besides the computational effort, these quantities are only accessible in some software packages (e.g., ANSYS, ABAQUS, OpenSees). Ultimately, the derivatives of Nelson's method may lead to incorrect results if repeated poles are present. This is the case for double-symmetrical structures, such as towers, but several approaches are available in the literature to remedy this problem [14].

The finite difference method, in spite of its dependency on the step size, can be implemented straightforwardly. It merely requires the observed natural frequencies and the mode shape at the considered sensor locations, which can be extracted from most finite element packages, e.g., SOFiSTiK, SAP2000, ETABS, etc. However, the mode shape normalization requires special attention, as it is not in-built into the sensitivity computation. Depending on the application,

data-driven modal parameters may even be available for damaged states (e.g., if a series of non-destructive tests were performed beforehand), in which case they can be used for the sensitivity computation based on the finite difference method and no numerical model is required.

5 Conclusions

This article proposes a new method to analyze changes in boundary conditions, i.e., changes in prestress or support conditions, based on sensitivity-based statistical tests. The method can identify changes in boundary conditions during the active monitoring phase, but can also be applied to assess the performance of monitoring systems before damages occur. For that purpose, an approach is described on how to draw probability of detection curves for local damages based on global data-driven features, such as modal parameters. The main contribution is a step-by-step description on how to calculate the sensitivity vectors for changing boundary conditions based on finite element models. Moreover, the advantages and disadvantages of analytical and approximate derivate computations are critically discussed. In summary, the developed method can be applied based on standard software. While this paper showcases a numerical proof of concept study based on a two-span reinforced concrete bridge with 14.124 degrees of freedom, the application to a real bridge will be the subject of future work.

Acknowledgements
This research study is funded by dtec.bw – Digitalization and Technology Research Center of the Bundeswehr.

References

[1] H. Wenzel and D. Pichler, Ambient vibration monitoring. John Wiley & Sons, 2005
[2] M. Basseville, M. Abdelghani, and A. Benveniste, Subspace-based fault detection algorithms for vibration monitoring, Automatica, No 36 Vol 1, pp 101-109, 2000.
[3] S. Allahdadian, M. Döhler, C. Ventura, and L. Mevel, Towards robust statistical damage localization via model-based sensitivity clustering, Mechanical Systems and Signal Processing, 134, 106341, 2019.
[4] M. Döhler, L. Mevel, and F. Hille, Subspace-based damage detection under changes in the ambient excitation statistics, Mechanical Systems and Signal Processing, Vol 45, No 1, p 207–224, 2014.
[5] S. Greś, M. Döhler, P. Andersen, and L. Mevel. Subspace-based Mahalanobis damage detection robust to changes in excitation covariance. Structural Control and Health Monitoring, Vol 28, No 8, e2760, 2021.
[6] S. Greś, A. Mendler, N.-J. Jacobsen, P. Andersen and M. Döhler, Statistical damage detection and localization with Mahalanobis distance applied to modal parameters, Proceedings of the International Modal Analysis Conference in Vancouver, 2022.
[7] A. Mendler, M. Döhler, C. U. Grosse, Selection of damage-sensitive features based on probability of detection curves, Proceedings of the International Operational Modal Analysis Conference in Vancouver, 2022.
[8] M. Döhler and L. Mevel, Efficient multi-order uncertainty computation for stochastic subspace identification, Mechanical Systems and Signal Processing, Vol 38, No 2, pp 346-366, 2013.

[9] A. Mendler, M. Döhler, and C.E. Ventura, A reliability-based approach to determine the minimum detectable damage for statistical damage detection, Mechanical Systems and Signal Processing, Vol 154, 107561, 2021.
[10] M. I. Friswell and A. W. Lees, Resonance frequencies of viscously damped structures, Journal of Sound and Vibration, Vol 217, No 5, pp 950-959, 1995.
[11] K.-J. Bathe, Finite element procedures. K.J. Bathe, Watertown, United States, 2nd edition, 2014.
[12] M. I. Friswell and S. Adhikari, Derivatives of complex eigenvectors using Nelson's method. AIAA journal, Vol 38, No12, pp 2355-235, 2000.
[13] W. Heylen and P. Sas, Modal analysis theory and testing, Katholieke Universiteit Leuven, Leuven, Belgium, 1997.
[14] Z. Xu and B. Wu, Derivatives of complex eigenvectors with distinct and repeated eigenvalues, International journal for numerical methods in engineering, Vol 75, No 8, pp 945-963, 2008.